

**An RNA aptamer that distinguishes between closely related human influenza viruses and inhibits haemagglutinin-mediated membrane fusion**

Subash C. B. Gopinath,<sup>1</sup>† Tomokos Misono,<sup>1</sup>† Kazunori Kawasaki,<sup>1</sup> Takafumi Mizuno,<sup>2</sup> Masaki Imai,<sup>2</sup> Takato Odagiri<sup>2</sup> and Penmetcha K. R. Kumar<sup>1</sup>

<sup>1</sup>Institute for Biological Resources and Functions, National Institute of Advanced Industrial Science and Technology, Central 6, 1-1 Higashi, Tsukuba City, Ibaraki 305-8566, Japan

<sup>2</sup>Department of Virology III, National Institute of Infectious Diseases, 4-7-1 Gakuen, Musashimurayama, Tokyo 208-0011, Japan

**Correspondence**

Penmetcha K. R. Kumar  
pkr-kumar@aist.go.jp

†These authors contributed equally to this work.  
Supplementary methods, figures and videos are available.

**Aptamers selected against various kinds of targets have shown remarkable specificity and affinity, similar to those displayed by antibodies to their antigens. To employ aptamers as genotyping reagents for the identification of pathogens and their strains, *in vitro* selections were carried out to find aptamers that specifically bind and distinguish the closely related human influenza A virus subtype H3N2. The selected aptamer, P30-10-16, binds specifically to the haemagglutinin (HA) region of the target strain A/Panama/2007/1999(H3N2) and failed to recognize other human influenza viruses, including another strain with the same subtype, H3N2. The aptamer displayed over 15-fold-higher affinity to the HA compared with the monoclonal antibody, and efficiently inhibited HA-mediated membrane fusion. These studies delineate the application of aptamers in the genotyping of viruses.**

## INTRODUCTION

*In vitro* genetic selection has allowed the isolation of nucleic acids that can bind target molecules with high affinity and specificity (Burgstaller *et al.*, 2002; Clark & Remcho, 2002; Göringer *et al.*, 2003; Nimjee *et al.*, 2005). The strategy involves the isolation of rare nucleic acid molecules that have high affinity for a target molecule from a pool of random nucleic acids, with subsequent repeated rounds of selection and amplification. This procedure has proved to be extremely useful for the isolation of tight-binding aptamers against a wide variety of targets, including metal ions, sugars, peptides, proteins and even whole cells. The binding affinities displayed by various aptamers to their cognate molecules are comparable to or higher than the affinities achieved by antibodies for antigens. Therefore, aptamers have been exploited for various kinds of applications *in vitro* and *in vivo*, including the detection and quantification of analytes and the inhibition of protein function or activity (decoy strategy), as well as in imaging processes and gene regulation. Moreover, the aptamers are known for their higher discriminating ability between closely related molecules and they require only a small region for binding, compared with an antibody. For example, the theophylline aptamer discriminates against caffeine by over 14 000-fold, even though the caffeine molecule differs from theophylline by only the presence of a methyl group at the N7 position (Jenison *et al.*, 1994).

In general, the aptamers require fewer residues to bind to the target proteins than their counterpart, antibodies, in which a group of six to eight amino acid residues (patch) or a larger surface area is required to interact with an antigen or protein. Although this perspective is based on the few available structures of aptamer–ligand and antigen–antibody complexes, if this notion is true for the aptamers, then these high-affinity motifs will be a very valuable tool to discriminate between closely related proteins or strains of micro-organisms. We sought to evaluate the ability of aptamers to distinguish between closely related organisms or pathogens by using whole viruses. As a test case, we chose two strains of human *Influenza A virus* [A/Panama/2007/1999(H3N2) and A/Aichi/2/1968(H3N2)]. The influenza virus genome contains eight single-stranded RNA segments; the two membrane glycoprotein components are haemagglutinin (HA) and neuraminidase (NA). About 900 and 300 copies of HA and NA, respectively, are expressed on the surface of each viral particle. HA is composed of disulfide-linked polypeptide chains, HA1 and HA2; the former is the major component of the HA antigen. The amino acid similarity for the HA1 subunit between influenza viruses is in the range 84–90 %. The differences in the HA1 primary sequences between the strains of the same subtype consist of stretches of point mutations with one to three residues, and stretches of four to six residues; however, some of these long stretches might not be exposed on the surface. The major viral antigen, HA, is required for membrane fusion with host cells to mediate the early stage of influenza virus infection (Skehel & Wiley, 2000). In addition, HA is known to induce high levels of macrophage-derived chemokines and cytokines, which lead to the infiltration of inflammatory cells and severe haemorrhaging, especially when the HA is derived from a virulent strain (Kobasa *et al.*, 2004). Previously, a DNA aptamer that blocks receptor binding has been reported (Jeon *et al.*, 2004).

At present, most of the commercially available monoclonal antibodies (mAbs) against HA cannot distinguish between viruses within the influenza subtypes. It is important to determine whether a highly pathogenic form of HA exists in an individual strain in addition to typing and subtyping the viruses, especially in a diagnostic scenario where the severity of an infectious agent must be predicted. In this study, we demonstrated that the selected aptamer has the ability to distinguish the viruses and, more specifically, to distinguish strains within subtypes of influenza type A viruses. The selected aptamer not only displayed a high discriminating ability for binding to the HA, but also showed higher affinity (over 15-fold) than the mAb. Furthermore, the selected aptamer efficiently inhibited HA-mediated membrane fusion.

## METHODS

***In vitro* selection of influenza A/Panama-specific binding aptamers.** To eliminate the RNAs that bound to the filter, the RNA pool was passed three times prior to each selection cycle through a pre-wetted nitrocellulose acetate filter (HAWP filter, 0.45  $\mu\text{m}$ , 13.0 mm diameter; Millipore) in 'Pop-top' filter holders (Nucleopore). To select specific binders, tRNA was used as a competitor during the entire selection process. For the first cycle of selection, approximately  $4 \times 10^{13}$  RNA sequences (in the N30 pool) in binding buffer [20 nM HEPES/KOH (pH 7.4), 105 mM NaCl] were denatured at 90 °C for 2 min and allowed to cool at room temperature for 10 min, to facilitate the equilibrium of different conformers. The pool RNAs and tRNA were combined, the whole virus, A/Panama/2007/1999(H3N2), was added and the final mixture [20 nM HEPES/KOH (pH 7.4), 105 mM NaCl, 7.8  $\mu\text{M}$  RNA pool, 9.3  $\mu\text{g}$  influenza A/Panama virus and 1.2  $\mu\text{M}$  tRNA as a competitor], in 50  $\mu\text{l}$  binding buffer, was incubated at room temperature for 30 min and filtered. The filter was washed with 1 ml binding buffer. The RNAs that were retained on the filter were eluted as described previously (Kumar *et al.*, 1997). The recovered RNAs were reverse-transcribed in 20  $\mu\text{l}$  reaction mixture, containing 50 mM Tris/HCl (pH 8.0), 40 mM KCl, 6 mM  $\text{MgCl}_2$ , 0.4 mM dNTPs, 2.5  $\mu\text{M}$  primer (24.N30) and 5 U AMV reverse transcriptase (Seikagaku). Nucleotides and enzymes were added after a denaturation and annealing step (2 min at 90 °C followed by an incubation at room temperature for 10 min). Reverse transcription was carried out for 1 h at 42 °C. For amplification by PCR, a 20  $\mu\text{l}$  aliquot of the mixture after reverse transcription (cDNA reaction mixture) was diluted in 80  $\mu\text{l}$  of a mixture for PCR [10 mM Tris/HCl (pH 8.8), 50 mM KCl, 1.5 mM  $\text{MgCl}_2$  and 0.1 % Triton X-100, 5 U *Taq* DNA polymerase (TaKaRa) and 0.4  $\mu\text{M}$  each of the 24.N30 and 39.N30 primers]. The reaction mixture was cycled at 94 °C for 1 min 15 s, 50 °C for 45 s and 72 °C for 1 min 15 s for as many cycles as needed to produce a band of product with the correct size. The PCR product was precipitated in ethanol and used for transcription. *In vitro* transcription was performed at 37 °C for 3 h with an AmpliScribe T7 kit (Epicentre Technologies) followed by a treatment with DNase I. The reaction mixture was fractionated on a 10 % denaturing polyacrylamide gel. The RNA was extracted from the gel, quantified and used for the next cycle of selection and amplification.

We manipulated each selection cycle to ensure specific and high-affinity binders to the A/Panama virus, including modifications of the ratio of RNA : virus, the competitor concentrations and the buffer volumes. To remove the filter-binding RNAs, we used xenobind plates for selection in the last two cycles. For the xenobind selection, we initially coated the wells with 9.75  $\mu\text{g}$  virus ( $\text{ml binding buffer}^{-1}$ ) and blocked the remaining sites with BSA (3 % stock solution). The wells were then washed and used in the selections. For the xenobind plate selections, the RNA pool from the eighth cycle was denatured at 90 °C for 2 min and allowed to cool at room temperature for 10 min, to facilitate the equilibrium of different conformers. Then, the pool RNA (0.5  $\mu\text{M}$ ) and tRNAs (5  $\mu\text{M}$ ), mixed in 200  $\mu\text{l}$  binding buffer, were loaded into the BSA-coated wells and were incubated for 10 min at room temperature (25 °C). The unbound RNAs were collected and loaded into the wells coated with the A/Aichi virus (9.75  $\mu\text{g ml}^{-1}$ ). The

reaction mixture was incubated further for 10 min. The unbound molecules were then collected and loaded into the wells coated with the A/Panama virus ( $9.75 \mu\text{g ml}^{-1}$ ). After this incubation, the wells were washed three times with  $300 \mu\text{l}$  binding buffer. The bound RNAs were recovered after a 20 min incubation with a hot ( $90 \text{ }^\circ\text{C}$ ) 7 M urea solution. The bound molecules were recovered by ethanol precipitation and regenerated by using PCR, RT and *in vitro* transcription. The tenth selection cycle was also repeated, using the above conditions except for an additional step of removing the A/Aichi binders, where the A/Aichi virus ( $3.2 \mu\text{g}$ ) was added, before recovering the A/Panama binders from the well with a hot 7 M urea solution.

**Inhibition of HA-mediated membrane fusion by the aptamer.** The potential inhibitory effects of RNA aptamers on HA-induced membrane fusion were examined by using fluorescently labelled virus and human red blood cell (RBC) ghost membranes. The viral membrane of A/Panama/2007/1999(H3N2) was labelled with a fluorescent lipid probe, octadecyl rhodamine B (R18; Molecular Probes) as described by Hoekstra *et al.* (1984). Human RBCs (type B+), obtained from a healthy donor, were washed three times with PBS and diluted to 1 % (v/v) in PBS. The RBCs ( $0.2 \text{ ml}$ ) were allowed to attach to a poly-L-lysine-coated glass coverslip at  $4 \text{ }^\circ\text{C}$  for 15 min and were then lysed to ghost membranes by three washes with ice-cold 5 mM sodium phosphate (pH 8.0). The ghost membranes were resealed in PBS containing 0.9 mM  $\text{CaCl}_2$  and 0.49 mM  $\text{MgCl}_2$  for 30 min at  $37 \text{ }^\circ\text{C}$  and were kept in PIPES buffer [5 mM PIPES/NaOH, 145 mM NaCl (pH 7.5)] on ice until use.

For the fusion-inhibition assay, an image analysis of fusion at single virions in the presence of RNA aptamers was performed as follows. The R18–A/Panama virus ( $0.05\text{--}0.1 \mu\text{g total protein ml}^{-1}$ ) mixed with an RNA aptamer, P30-10-16 (0.5 or 5  $\mu\text{M}$ ), in  $0.2 \text{ ml}$  PIPES buffer supplemented with an RNase inhibitor (1 U SUPERase-In  $\mu\text{l}^{-1}$ ; Ambion), was added to ghost membranes on coverslips mounted in a metal chamber (Mizuno *et al.*, 1992). After 3 min at  $20 \text{ }^\circ\text{C}$ , the unbound viral particles were removed by two washes with  $0.1 \text{ ml}$  PIPES buffer containing the RNase inhibitor (1 U  $\mu\text{l}^{-1}$ ) and the chamber was mounted on a laser-scanning microscope (LSM 510; Carl Zeiss) equipped with a Planapochromat 63/1.4 NA objective. Capturing of time-lapse sequences of the fluorescence images at 1.5 s intervals was started and then, to trigger the fusion activity of HA, the PIPES buffer was replaced with  $0.2 \text{ ml}$  acidic buffer [145 mM NaCl, 20 mM sodium citrate, 1 U RNase inhibitor  $\mu\text{l}^{-1}$  (pH 5.0)]. The fluorescence of R18 upon excitation with a 543 nm HeNe laser was imaged by using a 590 nm cut-off filter. To monitor the fluorescence intensities of individual fusing viral particles, regions of interest were drawn at the outlines of punctate fluorescence from R18–A/Panama viruses on each recorded image file. The changes in the fluorescence intensity at individual regions were measured with NIH Image 1.61 software. Upon viral fusion with ghost membranes, lipid intermixing between the viral and ghost membranes induced fluorescence dequenching of R18 (Georgiou *et al.*, 1989; Lowy *et al.*, 1990). Thus, the response times before the fusion of single viral particles were determined by the timing of fluorescence flashes at single regions of interest on the microscopic images. The kinetics of vesicle fusion were obtained from the cumulative sums of the response-time distributions.

## RESULTS AND DISCUSSION

### Selection of RNA aptamers

Aptamers that can distinguish between closely related viruses are eagerly sought, because this kind of specific probe will facilitate the development of not only specific diagnostic reagents, but also tailor-made drugs against the specific genotype that caused the infection. In addition, such reagents would be useful for monitoring and forecasting influenza epidemics and especially for identifying the more severe forms of strains within subtypes. However, the currently available mAbs against HA are not able to discriminate between HA proteins within subtypes of influenza viruses. To develop reagents that can discriminate between closely related strains of influenza viruses, we used an *in vitro*-selection strategy. In the first selection cycle, about  $10^{14}$  RNA sequences (N30 pool) were allowed to bind to the A/Panama(H3N2) virus (9.3  $\mu$ g total viral protein was mixed with 7.8  $\mu$ M RNA) in a binding buffer in which the virus and protein retain their activities. In the subsequent selection cycles, the ratio between the virus and the RNAs (N30 pool and tRNA) was manipulated to increase the selection stringency (Table 1). To ensure the enrichment of specific aptamers against A/Panama(H3N2) virus, we carried out a cross-selection procedure from cycle 6, where the pool was initially allowed to bind to A/Aichi(H3N2) and then the unbound RNA molecules were used to bind to the A/Panama(H3N2) virus. The RNA molecules that bound to the A/Panama(H3N2) virus were eluted and then used in the next selection cycle, after regenerating the RNA molecules through a combination of amplifying enzymes. The progression of both the enrichment of high-affinity antiviral aptamers and the specificity was analysed by a filter-binding assay. Individual aptamers from the tenth cycle were cloned and sequences of 17 clones were classified into three major groups (Fig. 1a). The aptamers representing these groups were assayed for A/Panama virus binding in the presence of a 10-fold molar excess of tRNA, for specific binding. The primary sequences of the RNA aptamers were folded, using the BayesFold program (version 1.01) to predict the possible secondary structures (Knight *et al.*, 2004) (Fig. 1b).

### Binding analysis of RNA aptamers to influenza viruses

Among the 17 clones sequenced from the pool, two main classes emerged. One class was represented at a lower frequency, whereas one sequence dominated in the other class, with about 50 % representation. Aptamers representing each group were analysed directly for binding to the A/Panama virus, using a filter-binding assay. Some of the aptamers were retained on the filter, but lacked protein-dependent binding. However, two kinds of aptamers, motif 1 (Fig. 2a) and motif 2 (data not shown), bound specifically to the A/Panama virus. Next, to examine the binding sites of the aptamers [motif 1 (P30-10-16) and motif 2 (P30-10-1)] in the A/Panama virus, we analysed their binding to the membrane proteins HA and NA, isolated from the A/Panama virus. The purity of these proteins was confirmed by cognate mAbs (data not shown). The binding activity of aptamers was analysed by filter-binding assay, similar to that used in the above studies; both aptamers bound to the HA of A/Panama virus with high affinity and specificity (Fig. 2a; P30-10-1 binding not shown). On the other hand, the motif 1 and motif 2

aptamers failed to bind to HA purified from A/Aichi virus, although the HA of A/Aichi virus shares about 84 % similarity in its primary amino acid sequence with that of A/Panama virus (Fig. 2b). Similarly, the binding ability of the dominant motif (motif 1) to other influenza viruses or HA was analysed, which confirmed that motif 1 bound specifically to the HA derived from A/Panama virus (Fig. 2c). The results suggested that these aptamers were specific for the HA of the A/Panama virus and were able to distinguish this HA from those of other influenza viruses, even including strains of the same subtypes. RNA motifs 1 and 2 appeared to discriminate the A/Panama virus with equal efficiency, based on the binding analysis.

### **Surface plasmon resonance (SPR) studies**

To determine the binding kinetics of the P30-10-16 aptamer–HA complex, we performed SPR studies (Supplementary Fig. S1). These studies revealed that the aptamer binds to HA with association ( $k_{on}$ ) and dissociation ( $k_{off}$ ) constants of  $2.1 \times 10^5 \text{ M}^{-1} \text{ s}^{-1}$  and  $3.4 \times 10^{-5} \text{ s}^{-1}$ , respectively. The equilibrium-dissociation constant ( $K_d$ ) for the above complex was 188 pM. However, the substitution of a complementary sequence within the random region of the P30-10-16 aptamer abolished the HA-binding ability, suggesting the importance of the sequence within this region. Next, to clarify the important region within the aptamer and to define the consensus RNA sequence for HA binding, we partially randomized the P30-10-16 aptamer sequence and found a consensus recognition motif specific for the HA of A/Panama virus. This motif was 5'-GUCGNC(N)<sub>4-5</sub>GUA-3' (where N indicates any base) (Misono & Kumar, 2005). Interestingly, the consensus sequence identified in these studies was located in the single-stranded region of the P30-10-16 aptamer, as predicted by the BayesFold program (version 1.01) (Knight *et al.*, 2004).

### **Analysis of the HA-binding region in the aptamer: mapping a minimal RNA motif that binds the HA of A/Panama virus**

To identify the important phosphates of the P30-10-16 aptamer and to derive shorter aptamers for the various analyses and applications, we used ethylnitrosourea (ENU)-modification and interference-analysis studies. Initially, the selected aptamer was labelled at the 5' end and modified under denaturing conditions (92 °C for 2 min) with ENU. Under these conditions, ENU modifies the phosphates of the RNA at approximately one site per molecule. As ENU reacts with phosphates and generates a phosphotriester in the RNA, it can be hydrolysed easily by a mild alkali treatment. The alkylated RNA was allowed to bind to HA and the complexed RNAs were separated from the free RNA by filtration and cleaved at the modified sites. The RNAs eluted from the nitrocellulose filters were loaded on a 10 % polyacrylamide gel to separate the cleaved products. In this process, the molecules that were modified at the phosphates necessary for binding to HA were lost and these important phosphate regions could be visualized as a footprint on the sequencing gel. Comparisons of the band intensities of the samples of complexed and free RNA revealed the sites that were important for HA binding. Specifically, the phosphates at positions 32, 34, 35, 37 and 39–43 were found to interfere with HA binding, suggesting their importance for interactions with HA (Fig. 3). Interestingly, all of

these critical phosphate residues were located in the single-stranded loop region, which coincided with the region of the general recognition motif mentioned above. Although the base sequences were optimized during the selection, the phosphates in the random regions might also play an important role in efficient binding to HA. Considering both the ENU-mapping and the doping-selection studies, we prepared a shorter derivative of the P30-10-16 aptamer containing nucleotide region 21–54 by using *in vitro* transcription and analysed the binding of the derivative to the HA of the virus, using the filter-binding assay. The shorter variant retained the HA-binding ability (data not shown). Taken together, these results clearly indicated that nt 21–54 of P30-10-16 were sufficient for binding to the A/Panama virus or its HA.

Aptamers reportedly have similar or higher affinity to their cognate target than do antibodies (Osborne *et al.*, 1997). This difference could originate during the binding reaction, at either the on rate (association constant) or the off rate (dissociation constant). As a mAb is commercially available against the same target, HA of A/Panama(H3N2) virus, we compared the kinetics of HA binding to the mAb and to the P30-10-16 aptamer by SPR analysis. This analysis revealed that the aptamer had about 15-fold-higher affinity than the mAb. The association ( $k_{on}$ ) and dissociation ( $k_{off}$ ) constants of the antibody–HA complex were  $2.3 \times 10^5 \text{ M}^{-1} \text{ s}^{-1}$  and  $6.6 \times 10^{-4} \text{ s}^{-1}$ , respectively. The equilibrium-dissociation constant ( $K_d$ ) for the above complex was 2.9 nM (Supplementary Fig. S2). A comparison of the association- and dissociation-rate constants suggested that the observed difference in the equilibrium-dissociation constants between the two kinds of complexes was due to the dissociation process. The aptamer–HA complex appeared to dissociate from the HA more slowly than the mAb–HA complex. This could be due to differences in their recognition modes: the RNA–protein interaction uses an ‘induced-fit’ mode, whereas the antibody–protein interaction uses a ‘lock-and-key’ docking mode.

### **Inhibition of HA-mediated membrane fusion by the aptamer**

As the selected aptamer has high affinity for the HA of influenza, it is important to analyse the ability of the aptamer to inhibit the biological functions of HA. It is known that the HA of influenza virus mediates membrane fusion between viral and target cellular membranes (Skehel & Wiley, 2000). Therefore, we analysed the interaction of fluorescently labelled virus and a model target membrane, RBC ghosts, in the presence of the aptamer P30-10-16 and the complementary RNA P30-10-16C, which would allow us to evaluate the ability of the aptamers to inhibit HA-mediated membrane fusion.

For a single-particle image analysis of membrane fusion, conjugates of R18–A/Panama virus and RBC ghosts were observed by fluorescence microscopy. As shown schematically in Fig. 4(a), viral membrane fusion with RBC ghosts induced lipid mixing between the two membranes and reduced the R18 concentration in the membranes. The change was detected as an increase in the intensity of R18 fluorescence from individual virus particles, as demonstrated previously (Georgiou *et al.*, 1989; Lowy *et al.*, 1990). Under approximately neutral-pH conditions (pH 7.5), individual virus particles were discerned as points of

fluorescence, whereas the RBC ghosts bound to the viruses were invisible (the first frames in Supplementary Videos S1 and S2). In the presence of the complementary RNA P30-10-16C (5  $\mu$ M), a low-pH trigger (pH 5.0) at 20 °C induced lateral diffusion of R18 from the viruses to the RBC ghosts, and the RBC ghosts became fluorescent within 300 s (Supplementary Video S1). Fig. 4(b) shows the time course of fluorescence intensity, recorded at a representative virus-particle region in the presence of P30-10-16C (5  $\mu$ M). In this case, an abrupt increase in the fluorescence was observed 80 s after the low-pH trigger, indicating that the particle caused membrane fusion (lipid mixing) with the RBC ghost after a response time of 80 s.

By contrast, in the presence of the aptamer P30-10-16 (5  $\mu$ M), lateral diffusion of R18 from the viruses to the RBC ghosts was not observed for most of the virus-ghost conjugates (Supplementary Video S2). Fig. 4(c) shows the time course of the fluorescence intensity recorded at a representative virus-particle region in the presence of P30-10-16 (5  $\mu$ M), demonstrating the absence of an abrupt increase in fluorescence, i.e. the absence of viral fusion.

The time distribution of fusion events, thus measured, was accumulated for several viral-particle regions and was used to obtain the viral fusion kinetics, as shown in Fig. 4(d). The efficiency of viral fusion with RBC ghosts 300 s after a low-pH trigger reached 79 % without the addition of any RNA and 85 % in the presence of 5  $\mu$ M P30-10-16C [Fig. 4(d), (i) and (ii)]. By contrast, in the presence of 0.5 and 5  $\mu$ M concentrations of the P30-10-16 aptamer, the viral fusion efficiencies were suppressed to 30 and 5 %, respectively [Fig. 4(d), (iii) and (iv)], showing the efficient inhibition of viral fusion by P30-10-16.

### **Analysis of aptamer-binding ability to HA derived from closely related H3N2 strains**

The above studies suggested that the aptamer discriminates between the two strains of influenza viruses (Panama and Aichi). However, the HA of A/Aichi, in terms of antigenicity and sequence evolution, is about as far as one can get from A/Panama within human H3 subtypes. Nevertheless, it would be of greater significance if the aptamers were able to discriminate HA derived from more closely related H3 isolates. To address this issue, we selected three more strains of H3 isolates [A/Wyoming/3/2003, A/Sydney/05/97 and A/Wuhan/359/95] and isolated the HA from these strains. The purity of HA preparations was verified by using mAb and they were tested for binding with aptamer (P30-10-16 mini) by using the SPR method mentioned above. The results show that HA derived from the A/Wyoming/3/2003 influenza strain is able to be recognized efficiently by the aptamer (Fig. 5). On the other hand, HA derived from the A/Sydney/05/97 or A/Wuhan/359/95 strains failed to be recognized by the aptamer, even at higher concentrations (500 nM) (Fig. 5). These differences in binding could originate from the loss of important contacting residues of HA derived from the latter two strains. These analyses suggest not only that the selected aptamer has the ability to distinguish closely related strains of viruses, but also suggest a possible binding site for the aptamer within the HA.

To identify potential residues of HA that are responsible for recognition of the aptamer, we have compared the primary sequences of HA derived from all five strains. Especially, aa 57, 142, 144, 172 and 192 were found to differ commonly at these positions, when compared

between the HA derived from strains recognized by the aptamer (Fig. 6). These residues are highlighted in Fig. 6 by an arrow and sphere. Interestingly, all of these residues are located on the surface of the HA molecule, facing towards solvent, based on the crystal structure of HA derived from A/Aichi/68(H3N2) (PDB accession no. 1HTM) (Fig. 7a, b). Among these, four residues are located within the loop regions (57, 142, 144 and 172) and only one residue is located within the  $\alpha$ -helix region. The HAs derived from the Panama and A/Wyoming/3/2003 strains have substitutions of G142R, G144N and D172E, to which the aptamer binds efficiently. These substitutions in these two strains may not only help in stabilizing the respective loops, but also allow interaction with the aptamer. Previously, such residues have been exploited by the RNA for binding to proteins (Matsugami *et al.*, 2003; Kumarevel *et al.*, 2005). Taken together, the above *in silico* analyses suggest that R142, N144 and E172 of HA from the Panama and Wyoming strains may interact with the aptamer. Nevertheless, the aptamer's ability to bind to other influenza strains of A/H3N2 having such substitutions, as well as structural studies on the HA–aptamer complex, indeed, reveals detailed interactions of the aptamer with HA.

## **ACKNOWLEDGEMENTS**

This work was supported by funds from the National Institute of Industrial Science and Technology to P. K. R. K; S. C. B. G is supported by the Japan Society for the Promotion of Science. We thank Dr Hideaki Kumihashi for a kind gift of purified virus and Ms Hiromi Masuda and Ms Takako Seki for the sequencing and the fusion analysis, respectively.

## REFERENCES

- Burgstaller, P., Jenne, A. & Blind, M. (2002).** Aptamers and aptazymes: accelerating small molecule drug discovery. *Curr Opin Drug Discov Devel* **5**, 690–700.
- Clark, S. L. & Remcho, V. T. (2002).** Aptamers as analytical reagents. *Electrophoresis* **23**, 1335–1340.
- Georgiou, G. N., Morrison, I. E. G. & Cherry, R. J. (1989).** Digital fluorescence imaging of fusion of influenza virus with erythrocytes. *FEBS Lett* **250**, 487–492.
- Göringer, H. U., Homann, M. & Lorgner, M. (2003).** In vitro selection of high-affinity nucleic acid ligands to parasite target molecules. *Int J Parasitol* **33**, 1309–1317.
- Hall, T. A. (1999).** BioEdit: a user-friendly biological sequence alignment editor and analysis program for Windows 95/98/NT. *Nucleic Acids Symp Ser* **41**, 95–98.
- Hoekstra, D., de Boer, T., Klappe, K. & Wilschut, J. (1984).** Fluorescence method for measuring the kinetics of fusion between biological membranes. *Biochemistry* **23**, 5675–5681.
- Jenison, R. D., Gill, S. C., Pardi, A. & Polisky, B. (1994).** High-resolution molecular discrimination by RNA. *Science* **263**, 1425–1429.
- Jeon, S. H., Kayhan, B., Ben-Yedidia, T. & Arnon, R. (2004).** A DNA aptamer prevents influenza infection by blocking the receptor binding region of the viral hemagglutinin. *J Biol Chem* **279**, 48410–48419.
- Knight, R., Birmingham, A. & Yarus, M. (2004).** BayesFold: rational 2° folds that combine thermodynamic, covariation, and chemical data for aligned RNA sequences. *RNA* **10**, 1323–1336.
- Kobasa, D., Takada, A., Shinya, K. & 16 other authors (2004).** Enhanced virulence of influenza A viruses with the haemagglutinin of the 1918 pandemic virus. *Nature* **431**, 703–707.
- Kumar, P. K. R., Machida, K., Urvil, P. T., Kakiuchi, N., Vishnuvardhan, D., Shimotohno, K., Taira, K. & Nishikawa, S. (1997).** Isolation of RNA aptamers specific to the NS3 protein of hepatitis C virus from a pool of completely random RNA. *Virology* **237**, 270–282.
- Kumarevel, T., Mizuno, H. & Kumar, P. K. R. (2005).** Structural basis of HutP-mediated anti-termination and roles of the Mg<sup>2+</sup> ion and L-histidine ligand. *Nature* **434**, 183–191.
- Lowy, R. J., Sarkar, D. P., Chen, Y. & Blumenthal, R. (1990).** Observation of single influenza virus–cell fusion and measurement by fluorescence video microscopy. *Proc Natl Acad Sci U S A* **87**, 1850–1854.
- Matsugami, A., Kobayashi, S., Ouhashi, K., Uesugi, S., Yamamoto, R., Taira, K., Nishikawa, S., Kumar, P. K. R. & Katahira, M. (2003).** Structural basis of the highly efficient trapping of the HIV Tat protein by an RNA aptamer. *Structure* **11**, 533–545.
- Misono, T. S. & Kumar, P. K. R. (2005).** Selection of RNA aptamers against human influenza virus hemagglutinin using surface plasmon resonance. *Anal Biochem* **342**, 312–317.
- Mizuno, T., Kawasaki, K. & Miyamoto, H. (1992).** Construction of a thermotaxis chamber providing spatial or temporal thermal gradients monitored by an infrared video camera system. *Anal Biochem* **207**, 208–213.
- Nimjee, S. M., Rusconi, C. P. & Sullenger, B. A. (2005).** Aptamers: an emerging class of therapeutics. *Annu Rev Med* **56**, 555–583.

**Osborne, S. E., Matsumura, I. & Ellington, A. D. (1997).** Aptamers as therapeutic and diagnostic reagents: problems and prospects. *Curr Opin Chem Biol* **1**, 5–9.

**Skehel, J. J. & Wiley, D. C. (2000).** Receptor binding and membrane fusion in virus entry: the influenza hemagglutinin. *Annu Rev Biochem* **69**, 531–569.

(a)

**Motif 1 (47 %)**

P30-10-16: 5'-GGGAGAAUCCGACCAGAAG GGUAGCAGUCGGCAUGCGGUACAGACAGA CCUUUCCUCUCUCCUCCUCUUCU-3'

**Motif 2 (18 %)**

P30-10-1: 5'-GGGAGAAUCCGACCAGAAG AAUAGUAGAAUGAGCUCUGUCGGACCCAG CCUUUCCUCUCUCCUCCUCUUCU-3'

**Other motifs**

P30-10-4: 5'-GGGAGAAUCCGACCAGAAG CUAUGGAGGUGGUGGUGGAUGCUCUGGUUG CCUUUCCUCUCUCCUCCUCUUCU-3'  
P30-10-9: 5'-GGGAGAAUCCGACCAGAAG GAUUGGUACUUAUGGAGGUGGUAUAGUA CCUUUCCUCUCUCCUCCUCUUCU-3'  
P30-10-10: 5'-GGGAGAAUCCGACCAGAAG AUUAUGCAGUUUCAUUAUAUCAACACCAA CCUUUCCUCUCUCCUCCUCUUCU-3'  
P30-10-13: 5'-GGGAGAAUCCGACCAGAAG CUCAUGGAGGUGGUGGCGAGCUUCAGGUG CCUUUCCUCUCUCCUCCUCUUCU-3'  
P30-10-14: 5'-GGGAGAAUCCGACCAGAAG CUCAUGGAGGUGGUGGAGUCUCUUGGUCA CCUUUCCUCUCUCCUCCUCUUCU-3'  
P30-10-15: 5'-GGGAGAAUCCGACCAGAAG GACAUUGUUGUAAUUUCGCCUAAGCCUAUC CCUUUCCUCUCUCCUCCUCUUCU-3'

(b)

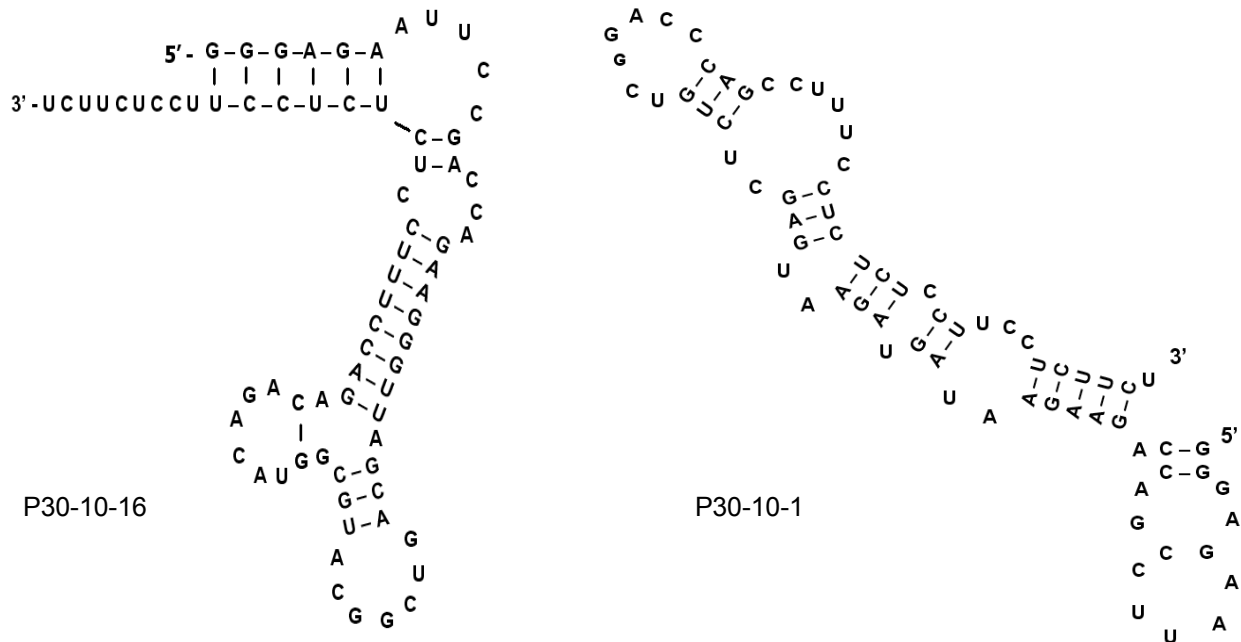


**Fig. 1.** (a) Primary sequences of selected aptamers against whole influenza virus. Underlined letters indicate the randomized region of the RNA. (b) Predicted secondary structures of the selected aptamers using BayesFold version 1.01.



**Fig. 3.** (a) ENU mapping of interfering phosphates of the selected aptamer and HA binding. The labelled, ENU-modified aptamer–HA complex was trapped on a nitrocellulose filter. After washing the complex with binding buffer, the filter was treated with mild alkaline solution and the RNA was recovered and loaded on the gel. Control RNA marker was prepared by partial nuclease digestion with RNase T1. Lane 1, T1 (0.1 U); lane 2, T1 (0.01 U); lane 3, alkali digestion; lane 4, ENU RNA in the absence of HA; lane 5, ENU RNA in the presence of HA. (b) Interfering phosphates of the aptamer and derived minimal RNA motif. Interfering phosphates are indicated by arrowheads.

**Fig. 4.** Inhibition of HA-mediated membrane fusion. The inhibitory effect of the RNA aptamer on HA-mediated fusion was examined by using a virus–RBC ghost fusion assay at pH 5.0 and 20 °C. (a) A schematic drawing of the detection of fusion at individual virus particles. Viral membranes of virus (A/Panama strain) were labelled with a fluorescent lipid probe, R18. Low pH-dependent viral fusion with the target membranes, RBC ghosts, induces intermembrane lipid mixing and dequenching of R18 fluorescence. The increase in the fluorescence intensity at an individual virus particle was observed by fluorescence microscopy. (b) Representative fluorescence-intensity data from a single virus region in the presence of complementary RNA P3-10-16C (5  $\mu$ M). In this case, an abrupt increase in fluorescence, indicating the onset of viral fusion (marked  $\triangle$ ), was recorded 80 s after the low-pH trigger (at time zero, marked  $\blacktriangle$ ). (c) Representative fluorescence-intensity data from a single virus region in the presence of the aptamer P3-10-16 (5  $\mu$ M). Although the low-pH trigger was applied at time zero (marked  $\blacktriangle$ ), no abrupt increase in fluorescence was observed during the experiment for 300 s. (d) Kinetics of viral fusion were obtained by counting the number of fused virus particles at each time point: (i) without the addition of RNA; (ii) in the presence of 5  $\mu$ M complementary RNA P30-10-16C; (iii, iv) in the presence of 0.5 and 5  $\mu$ M aptamer P30-10-16, respectively. P30-10-16 inhibited the membrane fusion of virus–RBC ghost conjugates.

**Fig. 5.** Specificity of the P30-10-16 aptamer and interaction of closely related viral species of A/Panama/2007/1999(H3N2) by SPR measurements. Twenty microlitres (50 nM final concentration) aptamer was injected at a flow rate of  $2 \mu\text{l min}^{-1}$  for 10 min. Sensogram runs with HA of different, closely related species were injected into the flow cell at a flow rate of  $20 \mu\text{l min}^{-1}$  for 3 min.

	<b>1</b>				
<b>Aichi_seq</b>	<b>QDLP</b>	<b>GNDNSTATLC</b>	<b>LGHHAVPNGT</b>	<b>LVKTITDDQI</b>	
Syd_seq	.KI.	.....	.....	.....N...	
Wuhan_seq	.K..	.....	.....	.....N...	
Panama_seq	.K..	.....S...	.....	.....N...	
Wyoming_seq	.K..	.....	I.....	.....N...	
			<b>57</b>		
<b>Aichi_seq</b>	<b>EVTNATELVQ</b>	<b>SSSTGKICNN</b>	<b>PHRILDGIDC</b>	<b>TLIDALLGDV</b>	<b>HCDVFQNETW</b>
Syd_seq	.....	.....R..DS	.....EN.	.....P	...G...KE.
Wuhanseq	.....	.....R..DS	.....KN.	.....P	...G...KE.
Panama_seq	.....	.....R..DS	..Q....EN.	.....P	...G...KE.
Wyoming_seq	.....	.....G..DS	..Q....EN.	.....P	Q..G...KK.
					<b>142 144</b>
<b>Aichi_seq</b>	<b>DLFVERSKAF</b>	<b>SNEYPYDVPD</b>	<b>YASLRSLVAS</b>	<b>SGTLEFITEG</b>	<b>FTWTGVTQNG</b>
Syd_seq	.....Y	..C.....	.....	.....NN.S	.N....A...
Wuhanseq	.....Y	..C.....	.....	.....TN..	.N....A.D.
Panama_seq	.....Y	..C.....	.....	.....NN.S	.N....A...
Wyoming_seq	.....Y	..C.....	.....	.....NN.S	.N.A.....
					<b>172</b>
<b>Aichi_seq</b>	<b>GSNACKRGP</b>	<b>SGFFSRLNWL</b>	<b>TKSGSTYPVL</b>	<b>NVTMPNNDNF</b>	<b>DKLYIWGIHH</b>
Syd_seq	T.Y....SSI	KS.....	HQLKYK..A.	.....K.	.....V..
Wuhanseq	T.Y....SV	KS.....	H.LEYK..A.	.....K.	.....V..
Panama_seq	T.S....RSN	KS.....	HQLKYK..A.	.....EK.	.....VL.
Wyoming_seq	T.S....RSN	KS.....	.HLKYK..A.	.....EK.	.....V..
					<b>192</b>
<b>Aichi_seq</b>	<b>PSTNQEQTSL</b>	<b>YVQASGRVTV</b>	<b>STRRSQQTII</b>	<b>PNIGSRPWER</b>	<b>GLSSRISIW</b>
Syd_seq	...DSD...I	.A.....	..K....V.	.....V.	.I.....
Wuhanseq	...DSD...I	.....	..K....V.	.....V.	.I.....
Panama_seq	...DSD.I..	.A.....	..K....V.	.....V.	.V.....
Wyoming_seq	.V.DSD.I..	.A.....I..	..K....V.	....Y..RV.	DI.....
					<b>327</b>
<b>Aichi_seq</b>	<b>TIVKPGDVLV</b>	<b>INSNGNLIAP</b>	<b>RGYFKMRTGK</b>	<b>SSIMRSDAPI</b>	<b>DTCISECITP</b>
Syd_seq	.....I.L	...T.....	.....I.S..	.....	GK.N.....
Wuhanseq	.....I.L	...T.....	.....I.S..	.....	GN.N.....
Panama_seq	.....I.L	...T.....	.....I.S..	.....	GK.N.....
Wyoming_seq	.....I.L	...T.....	.....I.S..	.....	GK.N.....
					<b>327</b>
<b>Aichi_seq</b>	<b>NGSIPNDKPF</b>	<b>QNVNKITYGA</b>	<b>CPKYVKQNTL</b>	<b>KLATGMRNVP</b>	<b>EKQT</b>
Syd_seq	.....	.....R.....	..R.....	.....	.....
Wuhanseq	.....	.....R.....	..R.....	.....	.....
Panama_seq	.....	.....R.....	..R.....	.....	.....
Wyoming_seq	.....	.....R.....	..R.....	.....	.....

**Fig. 6.** Sequence similarity of HA proteins among H3N2 strains. The sequences were aligned by using the BioEdit software (Hall, 1999). HA residues 57, 142, 144, 172 and 192, which have substitutions to other amino acids in two strains [A/Panama/2007/1999 (H3N2) and A/Wyoming/3/2003], are indicated by the arrow and sphere.

**Fig. 7.** (a) Crystal structure of HA derived from A/Aichi/68(H3N2). The important residues are coloured with respect to the residues highlighted in Fig. 6. (b) A close view of HA showing potentially important residues for binding to the aptamer.

**Table 1.** Selection cycles and binding analysis with whole influenza virus

Cycle	Pool RNA ( $\mu\text{M}$ )	Competitor* ( $\mu\text{M}$ )	Virus ( $\mu\text{g}$ )	Binding activities†	
				A/Panama	A/Aichi
1	7.8	1.2	9.3	0.08	0.08
2	1.9	1.2	9.3		
3	1.9	2.4	4.6		
4	1.9	2.4	0.96		
5	1.0	10.0	0.46	2.8	0.28
6	0.1	0.1	3.2		
7	1.9	10.0	3.0		
8	1.9	10.0	0.3	23.6	5.4
9‡	0.5	5.0	0.98		
10‡	0.5	5.0	0.98		

\*tRNA.

†Filter-binding assay.

‡Microtitre plates used.